Journal for ImmunoTherapy of Cancer

Lactylation-driven MVP upregulation boosts immunotherapy resistance by inhibiting PD-L1 degradation in hepatocellular carcinoma

Shuang Liu ,[1] Yihui Pan ,[2] Wenjian Liu ,[3] Xiaoyun Bu ,[4] Ruonan Shao ,[3] Qi Wang,[1] Jun Wu,[1] Chen Wu,[1] Wenwei Hu,[1] Jun Xu,[1] Changping Wu,[1,5] Jingting Jiang [5,6]

To cite: Liu S, Pan Y, Liu W, *et al*. Lactylation-driven MVP upregulation boosts immunotherapy resistance by inhibiting PD-L1 degradation in hepatocellular carcinoma. *Journal for ImmunoTherapy of Cancer* 2025;**13**:e012230. doi:10.1136/jitc-2025-012230

► Additional supplemental material is published online only. To view, please visit the journal online (https://doi.org/10.1136/jitc-2025-012230).

SL, YP and WL contributed equally.

Accepted 27 August 2025

For numbered affiliations see end of article.

Correspondence to
Professor Jingting Jiang;
jiangjingting@suda.edu.cn

ABSTRACT

Background Hepatocellular carcinoma (HCC) is a prevalent malignancy and the third leading cause of cancer-related mortality worldwide. Immune checkpoint inhibitors (ICIs) have emerged as first-line therapies for advanced HCC, substantially improving clinical outcomes. However, resistance to ICIs remains a major therapeutic challenge. Lactylation, a recently identified post-translational modification, has been implicated in tumor progression, although its role in ICIs resistance in HCC remains unclear.

Methods Cytotoxicity assays, flow cytometry and orthotopic HCC mouse model were used to evaluate the effects of lactylation in remodeling the immune microenvironment. Chromatin immunoprecipitation sequencing and RNA sequencing were employed to identify lactylation-regulated gene profiles. Programmed cell death-ligand 1 (PD-L1) protein degradation was assayed by cycloheximide-chase analysis and ubiquitination assay. Interactions between major vault protein (MVP) and β-transducin repeat-containing protein (β-TrCP) were analyzed by co-immunoprecipitation experiments. Site-directed mutagenesis and truncation mutants were designed to determine binding sites of MVP-β-TrCP complex.

Results Elevated lactylation correlates with poor prognosis and ICIs resistance in patients with HCC. Inhibition of lactylation enhances $CD8^+$ T-cell infiltration and cytokine production. Multiomics analyses identify MVP as a lactylation-regulated factor that suppresses $CD8^+$ T cell-mediated antitumor immunity. Elevated MVP expression is associated with resistance to checkpoint blockade therapy. Mechanistic studies reveal that histone lactylation-induced MVP upregulation stabilizes PD-L1 by preventing β-TrCP-mediated proteasomal degradation. Pharmacological inhibition of lactylation restores ICIs sensitivity in orthotopic HCC mouse models.

Conclusions Our findings demonstrate that histone lactylation promotes ICIs resistance via MVP-dependent PD-L1 stabilization. Therefore, targeting lactylation in combination with programmed cell death protein-1/PD-L1 blockade offers a promising strategy to overcome immunotherapy resistance in HCC.

WHAT IS ALREADY KNOWN ON THIS TOPIC

⇒ Lactate accumulation in the immunosuppressive tumor microenvironment is one crucial driver to promote immune evasion and therapeutic resistance to immune checkpoint inhibitors (ICIs). Lactylation is a novel lactate-derived post-translational modification involved in multiple stages of tumorigenesis. However, the exact role of lactylation in hepatocellular carcinoma (HCC) progression, particularly in antitumor immunity, remains largely unknown.

WHAT THIS STUDY ADDS

⇒ High levels of lactylation are correlated with poor prognosis and ICIs resistance in patients with HCC. Inhibition of lactylation enhances $CD8^+$ cytotoxic T lymphocytes-mediated antitumor immunity. Mechanistically, H3K18la-induced major vault protein (MVP) upregulation stabilizes programmed cell death-ligand 1 (PD-L1) by preventing β-transducin repeat-containing protein (β-TrCP)-mediated proteasomal degradation. Pharmacological inhibition of lactylation restores ICIs sensitivity in orthotopic HCC mouse models.

HOW THIS STUDY MIGHT AFFECT RESEARCH, PRACTICE OR POLICY

⇒ Our findings reveal a novel mechanism of lactate-induced immune escape as well as the resistance of anti-programmed cell death protein-1/PD-L1 immunotherapy, offering critical insights for the development of combinatorial strategies aimed at overcoming immunotherapy resistance in HCC.

INTRODUCTION

Hepatocellular carcinoma (HCC) is one of the most prevalent malignancies worldwide and ranks as the third leading cause of cancer-related mortality, with a 5-year survival rate of approximately 18%.[1] In recent years, immune checkpoint inhibitors (ICIs) have revolutionized the therapeutic landscape for patients with advanced HCC.[2 3] However, only

fewer than 30% of patients with HCC exhibit a clinical response to ICIs due to insufficient immune activation.[4] The heterogeneity and unpredictability of immunotherapy resistance mechanisms remain a major obstacle in developing effective treatment strategies to overcome drug resistance and improve clinical outcomes of patients with advanced HCC.

Metabolic reprogramming is recognized as one of the essential hallmarks of cancer.[5] Increased glucose uptake and lactate production by tumor cells create an acidic and immunosuppressive microenvironment that promotes tumor progression.[6–8] Recently, lactate-derived lactylation of protein has been reported as a novel epigenetic modification that directly activates the transcription of gene involved in wound healing during M1 macrophage polarization.[9] The level of lactylation is modulated by intracellular lactate concentration in a dose-dependent manner.[10] Hypoxia, glycolysis and exogenous lactate can indirectly promote lactylation. Histone deacetylases function as lysine delactylases, whereas EP300 serves as a "writer" of lactylation in vivo.[9 11] Lactylation plays a pivotal role in HCC pathogenesis. Comprehensive lactylome profiling has shown that lactylation primarily impacts enzymes central to key metabolic pathways, including the tricarboxylic acid cycle, amino acid metabolism, fatty acid metabolism, and nucleotide metabolism.[12] SIRT3 has been shown to delactylate cyclin E2 at K348la, thereby inducing apoptosis in HCC.[13] Pan *et al* demonstrated that demethylzeylasteral suppressed tumorigenesis of liver cancer stem cells by disrupting histone lactylation associated with metabolic stress.[14] Nonetheless, the exact role of lactylation in HCC progression, particularly in antitumor immunity, remains incompletely understood.

Major vault protein (MVP), the primary structural component of cellular ribonucleoprotein particles known as vaults, forms large, hollow, barrel-shaped assemblies composed of two symmetrical halves.[15 16] The vault poly (ADP-ribose) polymerase, telomerase-associated protein-1, and several small untranslated RNAs are accumulated in the internal cavity of vaults.[17] Owing to their unique structure, vaults are involved in a range of biological processes, including proliferation, differentiation, signal transduction, drug resistance, and immune response.[18–23] However, little is currently known about the role of MVP in tumor immunity.

Our study reveals that global lactylation levels are elevated in patients with ICIs-resistant HCC and correlate with poor clinical outcomes. Histone lactylation upregulates MVP expression, which suppresses $CD8^+$ T cell-mediated antitumor immunity by blocking β-transducin repeat-containing protein (β-TrCP)-mediated proteasomal degradation of programmed cell death-ligand 1 (PD-L1). These findings suggest that co-targeting lactylation and immune checkpoints may enhance antitumor immune responses in HCC. Our findings offer critical insights for the development of novel combinatorial strategies aimed at overcoming immunotherapy resistance.

MATERIALS AND METHODS

Patients

Commercially available tissue microarray slides containing a total of 79 HCC samples and paired peritumoral tissues with clinical information and follow-up data were purchased from Outdo Biotech, Shanghai (Cohort 1). Ethical approval for the study of tissue microarray slides was granted by the Clinical Research Ethics Committee of Outdo Biotech. 28 patients with advanced HCC diagnosed at the Third Affiliated Hospital of Soochow University in 2019–2023 who had previously received anti-programmed cell death protein-1 (PD-1)/PD-L1 treatment were enrolled in this study. Among them, 19 patients were treated with sintilimab (200 mg, day 1, every 3 weeks) and the remaining 9 patients received atezolizumab (1,200 mg, day 1, every 3 weeks) treatment. All patients were treated with a combination of bevacizumab (15 mg/kg, day 1, every 3 weeks). Treatment was continued for at least two courses in the absence of drug intolerance. Tumor response was evaluated according to Response Evaluation Criteria in Solid Tumors V.1.1 guidelines. Among 28 patients, 8 of them achieved partial response (PR), 9 patients achieved stable disease (SD) and the remaining 11 patients were clinically assessed to have progressive disease (PD).

Mice

4–5 weeks old male C57BL/6 mice were purchased from the Vital River Laboratory (Beijing, China). All the mice were housed under specific-pathogen-free conditions. All procedures were approved by the Ethics Committee of Jiangsu Kerbio Medical Technology Group (Ethics approval number: IACUC25-0094). Animal suffering was minimized or prevented at all times to improve animal welfare.

For the orthotopic liver tumor model, 2×10^6 Hepa 1–6 cells stably transfected with luciferase in 20 µL of sterile serum-free Dulbecco's Modified Eagle's Medium (DMEM) (Cat#C11995500BT, Gibco) were injected into the left liver lobe of C57BL/6 mice. The tumor volume was calculated as length×width×width/2 and measured every 3 days. Treatments were started when tumors reached a volume of 100–150 mm^3. For lactate dehydrogenase inhibitor (LDHi) treatment experience, tumor-bearing mice were randomly divided into three groups and treated with oxamate (Cat#HY-W013032A, MCE, 500 mg/kg, intraperitoneal injection) or GSK2837808A (Cat#HY-100681, MCE, 6 mg/kg, oral) for 2 weeks (n=5), plus an untreated control. For in vivo animal studies to verify the functions of MVP, MVP-knockout and control Hepa 1–6 cells stably transfected with luciferase were both seeded at a density of 2×10^6 in 20 µL serum-free DMEM and then injected into the left liver lobe of C57BL/6 mice. CD8α monoclonal antibody (mAb) (Cat# BP0117, Bio X Cell) or the corresponding IgG2 isotype (Cat# BP0090, Bio X Cell) was administered intraperitoneally every 3 days after the tumor volume

reached 100–150 mm^3 at a concentration of 100 µg/mouse (n=5). For combination therapy, 2×10^6 Hepa 1–6 cells stably transfected with luciferase in 20 µL sterile serum-free DMEM were injected into the left liver lobe of C57BL/6 mice to develop orthotopic liver tumors. Treatments were initiated when tumors reached a volume of 100–150 mm^3. Tumor-bearing mice were randomly divided into four groups and treated with an intraperitoneal injection of anti-PD-1 mAb (Cat# BE0146, Bio X Cel, 200 µg/mouse i.p.) and oxamate (500 mg/kg i.p.), either individually or in combination (n=5), plus an untreated control. Tumor engraftment was assessed via bioluminescence imaging. At the end of the study, tumors were removed from the sacrificed mice and divided into two groups. Half of the tumors were lysed to obtain a single-cell suspension of tumor cells that were analyzed by flow cytometry. The remaining half was fixed in neutral buffered formalin (Cat# HT501128, Sigma-Aldrich), paraffin-embedded and sectioned for additional immunohistochemistry (IHC) pathological analysis.

Cell culture

HEK-293T cells, human HCC cells (Hep G2 and MHCC97-H), and a murine HCC cell line (Hepa 1–6) were obtained from the Cell Bank of the Chinese Academy of Sciences (Shanghai, China). Cell lines were maintained in DMEM supplemented with 10% fetal bovine serum (Cat# 10099–141, Gibco) and 1% penicillin-streptomycin (Cat# BL505A, Biosharp). Cells were cultured in a humidified atmosphere of 5% carbon dioxide at 37°C. All cells were authenticated by the short tandem repeat method and were checked for *Mycoplasma* contamination every 3 weeks.

Statistical analysis

Statistical analyses were performed using GraphPad Prism software (V.9.0) and SPSS software (V. 25.0). Two-tailed Student's t-test and one-way analysis of variance were applied for calculating statistical significance. Survival analysis was performed using Kaplan-Meier survival curves, and the comparison was performed using the log-rank test (Mantel-Cox test). Gene expression correlations were assessed using Pearson's correlation analysis. P value<0.05 was considered statistically significant (*p<0.05; **p<0.01; ***p<0.001; ****p<0.0001). All experiments were carried out with three biological replicates, unless otherwise indicated, and were presented as mean±SD.

More details of materials and methods are provided in online supplemental information.

Data availability statement

All data associated with this study are presented in the paper or the online supplemental data. The materials supporting the findings of this study are available from the corresponding author on reasonable request.

RESULTS

Elevated lactylation level is associated with poor survival and ICIs resistance in patients with HCC

Metabolic reprogramming is considered a hallmark of cancer and contributes to cancer progression. Gene Set Enrichment Analysis demonstrated a significant enrichment of gene signature correlated to glycolysis and lactate production in HCC samples (online supplemental figure 1A-C). Beyond its classical role as a metabolic by-product, lactate also serves as a substrate for the post-transcriptional modification of proteins. To investigate the clinical significance of lactylation in HCC, matched tumor and adjacent non-tumorous liver tissues were analyzed via IHC. The results revealed a significant elevation in global lactylation (pan-Kla) levels in HCC tissues compared with those in non-tumorous counterparts (figure 1A,B). Elevated pan-Kla levels were associated with advanced tumor stage, greater lesion number, and increased tumor size (figure 1C–E). Notably, patients who eventually developed SD and PD after anti-PD-1/PD-L1 therapy exhibited significantly higher lactylation levels compared with patients achieved PR (figure 1F,G). The response rate of anti-PD-1/PD-L1 therapy reduced dramatically in patients with high lactylation levels (figure 1H). High global lactylation levels were also relevant to shorter overall survival (OS) (figure 1I,J). To identify specific lactylation loci implicated in immunotherapy resistance, we quantified the level of lactylation on seven common lysine residues in histones. Among these, histone H3 lysine 18 lactylation (H3K18la) was markedly upregulated in patients who did not respond to anti PD-1/PD-L1 therapy (online supplemental figure 2A). Similar to pan-Kla, H3K18la was upregulated in HCC tissues and positively correlated with tumor burden and disease severity (online supplemental figure 2B-F). Importantly, high H3K18la levels may suggest non-responsiveness to ICIs therapy, with a shorter OS in patients with HCC (online supplemental figure 2G-J). These findings suggested that elevated lactylation levels, particularly H3K18la, predicted a more aggressive phenotype and may serve as a potential driver of immunotherapy resistance in HCC.

Inhibition of lactylation leads to increased infiltration of $CD8^+$ T cells with enhanced antitumor activity

Due to the lack of specific inhibitors of lactylation, we employed the lactate dehydrogenase inhibitor oxamate and GSK2837808A, which were previously reported to reduce lactate production and subsequently lower lactylation levels.[9] To explore the immunomodulatory effects of lactylation, naïve T cells were isolated from the spleens of C57BL/6 mice, activated with anti-CD3/CD28 beads, and then co-cultured with HCC cells. The addition of 10 mM lactate during in vitro culture significantly reduced the proportion of $CD3^+CD8^+$ T cells relative to phosphate-buffered saline-treated controls. Furthermore, lactate suppressed the expression of effector molecules, including interferon (IFN)-γ, tumor necrosis factor (TNF)-α, and granzyme B (GzmB), in $CD8^+$ T-cells

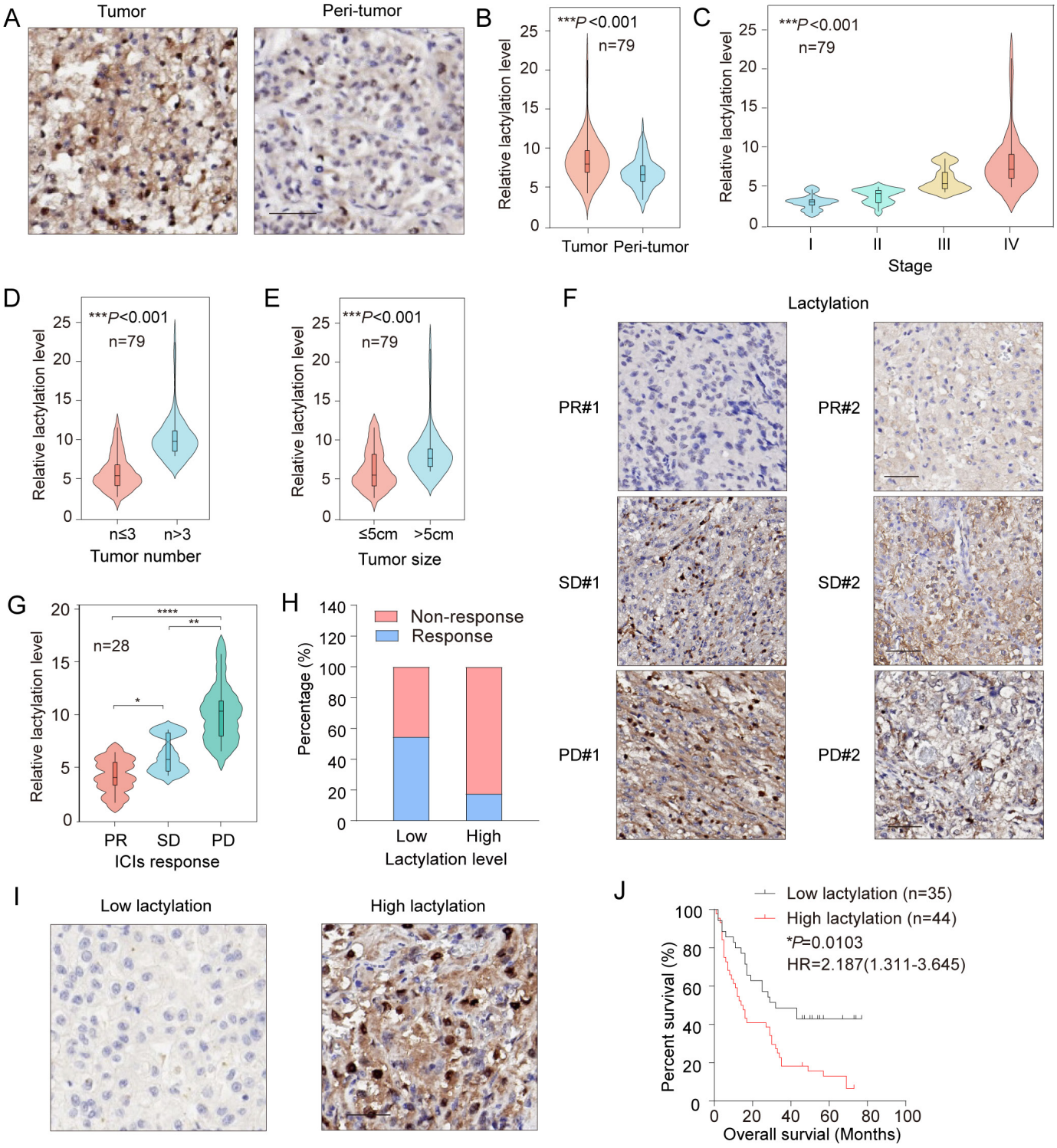

Figure 1 Elevated lactylation levels are associated with poor survival and ICIs resistance in patients with HCC. (A) Representative IHC images showing the levels of lactylation in HCC and paracarcinoma liver tissues (scale bar: 50 µm). (B) Statistical analysis of relative lactylation levels in 79 paired HCC and paracarcinoma liver tissues. (C–E) Relative lactylation levels in 79 HCC tissues classified according to the clinical stage (C), tumor number (D), and tumor size (E). (F) Representative IHC images showing different levels of lactylation in six patients with HCC treated with anti-PD-1/PD-L1 (scale bar: 50 µm). (G) Statistical analysis of relative lactylation levels in 28 patients with HCC treated with anti-PD-1/PD-L1. (H) Percentage of patients with HCC with PR or SD/PD after anti-PD-1/PD-L1 treatment in the low-lactylation or high-lactylation groups. (I) Two representative IHC images showing different levels of lactylation in human HCC tissues (scale bar: 50 µm). (J) Overall survival in patients with HCC with low or high lactylation levels was analyzed by Kaplan-Meier plots. *p<0.05, **p<0.01, ***p<0.001, ****p<0.0001. p<0.05 was considered statistically significant. HCC, hepatocellular carcinoma; ICIs, immune checkpoint inhibitors; PD, progressive disease; PD-1, programmed cell death protein-1; PD-L1, programmed cell death-ligand 1; PR, partial response; SD, stable disease.

(online supplemental figure 3A). In order to correct for pH-related effects on cell culture, we standardized the pH to 7.5 using NaOH in the lactate-treated groups. Despite this adjustment, the decline in $CD8^+$ T-cell subset and cytokine production persisted, supporting a pH-independent immunosuppressive role for lactate (online supplemental figure 3A). LDHi treatment modestly increased $CD8^+$ T-cell proportions and cytokine secretion in vitro, although the differences were not statistically significant (online supplemental figure 3B). Conversely, supplementation of pyruvate slightly reduced the $CD3^+CD8^+$ T-cell subset and cytokine production by elevating lactate levels, which could be partially rescued by co-administration of LDHi (online supplemental figure 3B).

We next established an orthotopic liver cancer model in C57BL/6 mice using the Hepa 1–6 cell line. LDHi treatment was initiated on day 14 following the inoculation and the mice were euthanized by day 30. At the end of the observation, the tumors were collected, and used for IHC analysis or for flow cytometry assay (figure 2A). Fluorescence living imaging showed the LDHi-treated tumors had a dramatically less vigorous fluorescence intensity than the control tumors (figure 2B,C). In line with these results, tumor weight was found to be lower in the treated group (figure 2D). LDHi treatment also markedly lowered lactate concentrations within the tumor microenvironment (TME) (figure 2E). Flow cytometric analysis was performed to investigate the immunological impact of LDHi. Notably, although LDHi had no discernible effect on the proportion of $CD8^+$ T-cell subsets in vitro, it significantly increased the infiltration of $CD8^+$ T cells within the TME in vivo, suggesting an enhanced antitumor immune response (figure 2F–H). We further evaluated the effect of LDHi on key effector cytokines, IFN-γ and TNF-α, which are critical for T-cell function. Flow cytometry confirmed a significant accumulation of IFN-γ^+ and TNF-α^+ $CD8^+$ T cells after LDHi treatment compared with controls (figure 2I). Analysis of immune checkpoint molecules expression showed that LDHi treatment decreased the proportion of PD-1^+ and TIM-3^+ $CD8^+$ T cells, while CTLA-4^+ $CD8^+$ T cells exhibited a modest increase (figure 2J). The attenuated lactylation and increased $CD8^+$ T-cell infiltration in LDHi-treated tumors were further verified by IHC (figure 2K,L). Collectively, our findings demonstrate that LDHi enhances $CD8^+$ T cell-mediated antitumor activity by reducing lactylation levels in the TME.

H3K18la regulates the transcription of MVP

To investigate the role of lactylation in HCC tumorigenesis, RNA sequencing (RNA-seq) was performed on human HCC cells following the treatment with LDHi (figure 3A). Functional enrichment analysis showed that differentially expressed genes were predominantly associated with cytokine signaling, cell adhesion and metabolic pathways (figure 3B). To further explore the epigenetic landscape regulated by lactylation, chromatin immunoprecipitation followed by sequencing (ChIP-seq) was conducted using pan-Kla antibody. Kyoto Encyclopedia of Genes and Genomes analysis demonstrated that genes with lactylation-enriched promoters were significantly involved in metabolic regulation, cell adhesion, and chemokine/cytokine signaling pathways (figure 3C). Integrative analysis of ChIP-seq and RNA-seq datasets identified four lactylation-regulated genes that were highly expressed in HCC (figure 3D). Among these, MVP emerged as one of the most remarkably downregulated genes on glycolysis inhibition (figure 3E). Previous studies have demonstrated that MVP is the key component of ribonucleoprotein complexes known as vaults. MVP participates in multiple cellular processes, including nucleocytoplasmic transport, signal transduction, drug resistance, cell differentiation, and immune responses.[24] We therefore focused further investigation on MVP. ChIP-seq analysis revealed a marked enrichment of lactylation signals at the MVP promoter (online supplemental figure 4A). Moreover, RNA-seq analysis from the Cancer Genome Atlas (TCGA) database showed a positive correlation between MVP expression and key glycolytic regulators—LDHA, LDHB, and SLC16A3 (online supplemental figure 4B-D). The positive correlation between lactylation levels and MVP expression was validated by histopathological analysis of patients with HCC (online supplemental figure 4E and F). TCGA database analysis also indicated that MVP expression was higher in tumor tissues compared with adjacent normal tissues (figure 3F). Patients with high MVP expression exhibited shorter OS compared with those with lower MVP expression (figure 3G). A similar trend was observed in another independent patient cohort (figure 3H,I). More importantly, patients who developed SD and PD after anti-PD-1/PD-L1 therapy exhibited significantly higher MVP expression compared with patients achieved PR (figure 3J). The response rate of anti-PD-1/PD-L1 therapy showed a reduction in patients with high MVP expression, suggesting a potential immunomodulatory role of MVP (figure 3K).

To elucidate the regulatory effects of lactylation on MVP expression, ChIP-quantitative PCR (qPCR) was employed to confirm enrichment of the MVP promoter in the DNA precipitated with the pan-Kla antibody, with particular emphasis on H3K18la-modified fragments (figure 4A–B). Similar enrichment patterns were observed in DNA precipitated with anti-EP300, a known “writer” of histone lactylation (figure 4C). ChIP-qPCR analysis further showed that LDHi treatment significantly reduced the binding of both H3K18la and EP300 at the MVP promoter (figure 4D,E). Detailed mapping of histone lactylation sites revealed strong H3K18la enrichment within the −995 to −1,501 nt region upstream of the MVP transcription start site, which was markedly diminished on LDHi treatment (figure 4F,G). As anticipated, LDHi treatment led to a significant reduction in both MVP messenger RNA (mRNA) and protein levels (figure 4H,I). In contrast, treatment with rotenone—a mitochondrial complex I inhibitor, enhanced MVP expression by inducing glycolysis (figure 4J). MVP upregulation was also observed

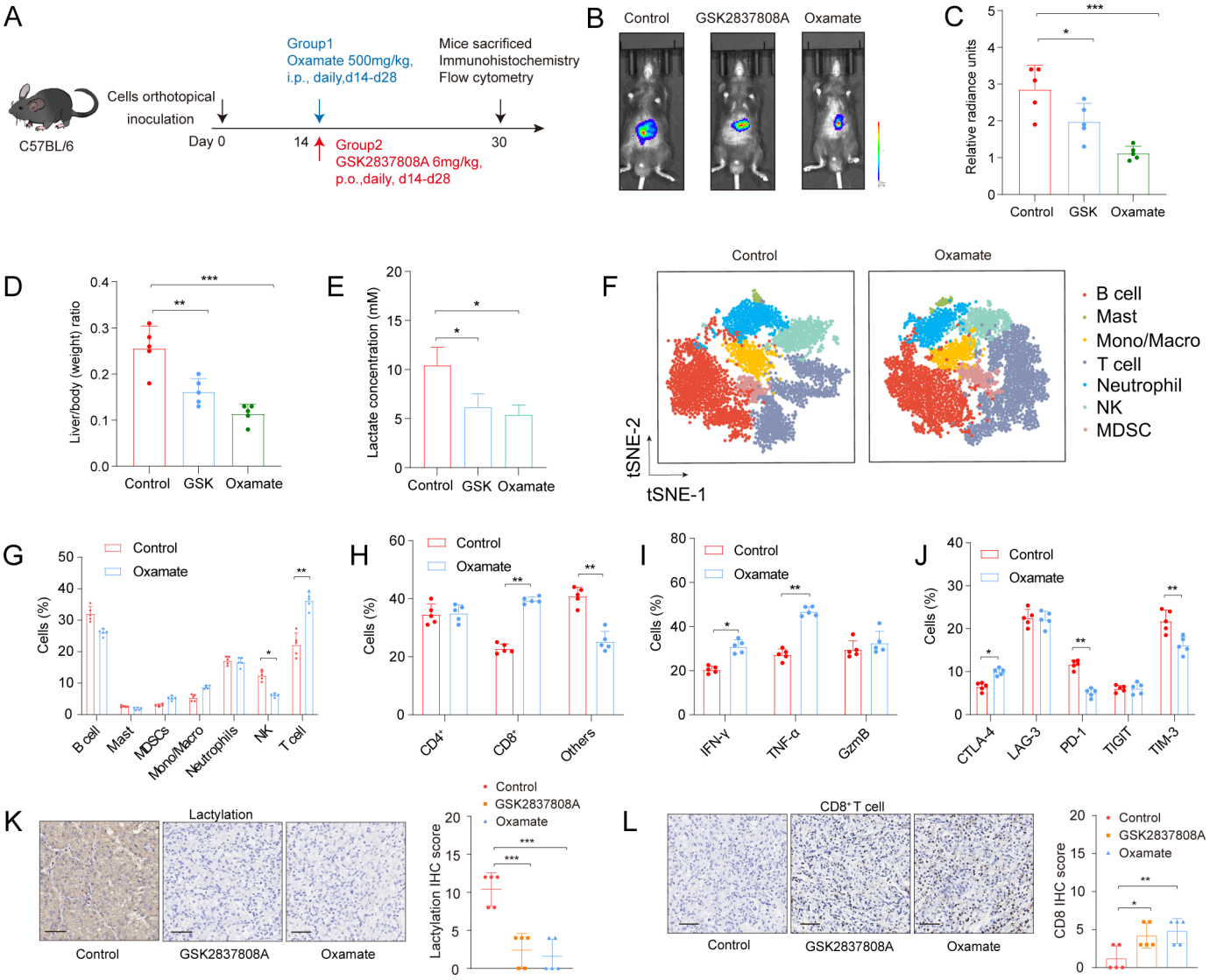

Figure 2 Inhibition of lactylation leads to increased infiltration of CD8⁺ T cells with enhanced antitumor activity. (A) Schematic diagram of animal experiments. (B) Representative fluorescence images of orthotopic HCC models in control and LDHi-treated group. (C) Relative radiance units in control and LDHi-treated group (n=5). (D) Weight of tumors was measured at the endpoint (n=5). (E) Lactate concentrations in TME of three groups of mice. (F–G) Subpopulations of immune cells in the TME were identified through flow cytometric analysis. (H) T-cell subclusters were analyzed throughflow cytometry. (I) Percentage of effector CD8⁺ T cells was evaluated through flow cytometry. (J) Expression of immune checkpoint molecules on CD8⁺ T cell was analyzed through flow cytometry. (K–L) Representative IHC images of lactylation (K) and tumor-infiltrating CD8⁺ lymphocytes (L) in the three groups (scale bar: 100 µm). *p<0.05, **p<0.01, ***p<0.001. p<0.05 was considered statistically significant. CTLA-4, cytotoxic T lymphocyte-associated protein 4; GzmB, granzyme B; HCC, hepatocellular carcinoma; IFN, interferon; IHC, immunohistochemistry; i.p.,intraperitoneal injection; LAG-3, lymphocyte activation gene-3; LDHi, lactate dehydrogenase inhibitor; MDSCs, myeloid-derived suppressor cells; NK, natural killer; PD-1, programmed cell death protein-1; TIGIT, T cell immunoreceptor with immunoglobulin and tyrosine-based inhibitory motif (ITIM) domain; TIM-3, T cell immunoglobulin and mucin-domain-containing-3; TME, tumor microenvironment; TNF, tumor necrosis factor; t-SNE,t-distributed stochastic neighbor embedding.

under hypoxic conditions, coinciding with increased expression of HIF-1α, MCT4, LDHA, and LDHB (online supplemental figure 4G). Furthermore, silencing EP300 via siRNA reduced both H3K18la and MVP protein levels, and abrogated lactate-induced MVP upregulation (online supplemental figure 4H and I). mRNA stability assays demonstrated that glycolysis inhibition did not affect the mRNA stability of MVP, suggesting transcriptional regulation as the primary mechanism (online supplemental figure 4J). Dual-luciferase reporter assay confirmed that lactate supplementation significantly increased MVP promoter activity, which was abolished by EP300 knockdown (online supplemental figure 4K). Conversely, LDHi attenuated the activity of the MVP promoter, which was reversed by exogenous lactate (online supplemental figure 4L). Taken together, these results suggest that lactate-induced H3K18la promotes MVP transcription through enhanced binding at its promoter.

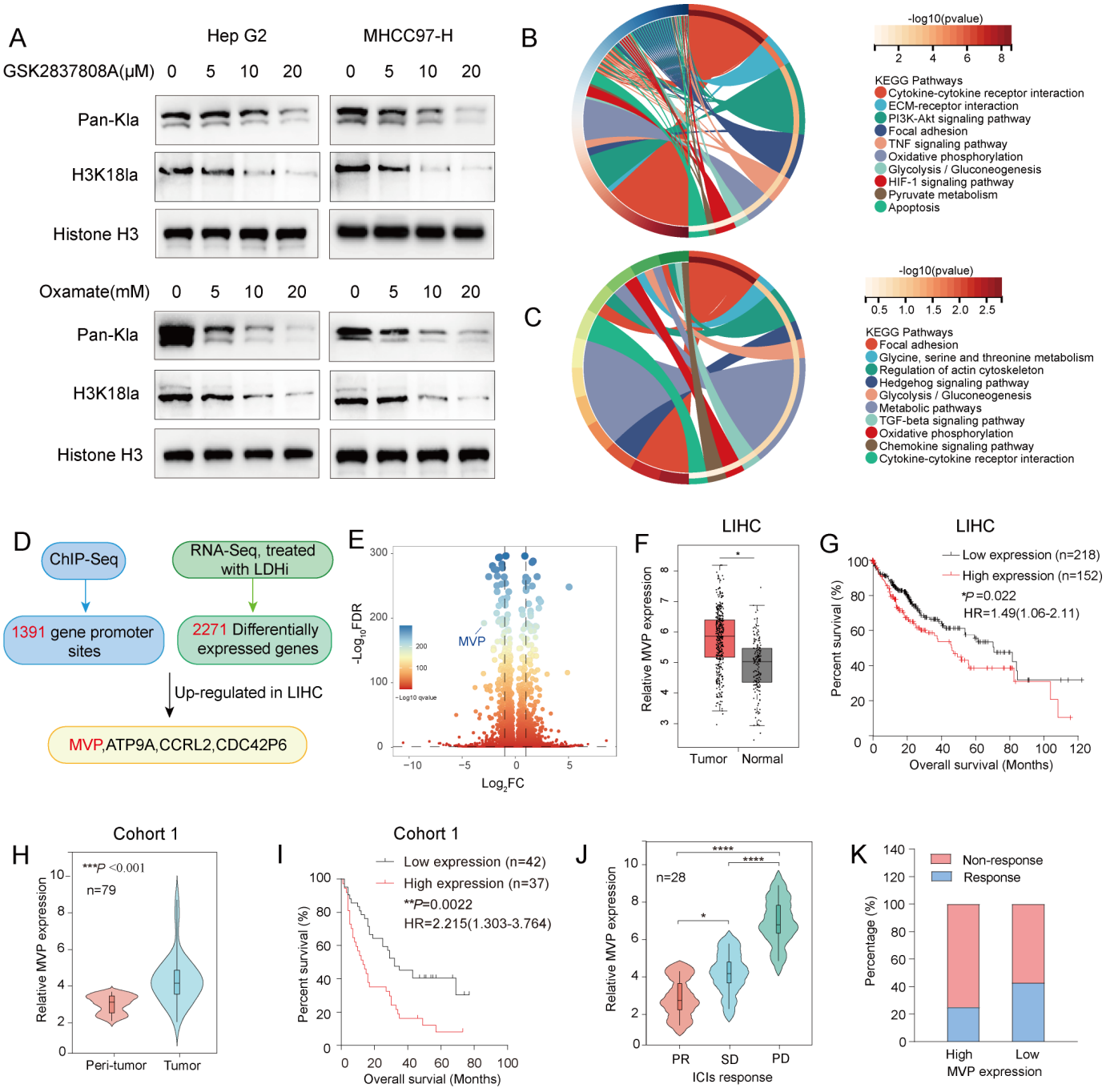

Figure 3 MVP is a downstream effector of histone lactylation. (A) Global lactylation and H3K18la levels were detected in Hep G2 (left) and MHCC97-H (right) cells after cultured in different concentrations of LDHi for 48 hours. (B) KEGG analysis of Hep G2 treated with LDHi. (C) KEGG analysis of lactylation-rich peaks after ChIP. (D) Workflow of selecting lactylation-regulated genes. (E) Volcano plot showed differentially-expressed genes after treatment with LDHi. Blue arrowhead indicated MVP. (F, H) Relative MVP expression in HCC tissues and normal liver tissues in LIHC (F) and Cohort 1 (H). (G, I) Overall survival of patients with HCC with low and high MVP expression was analyzed by Kaplan-Meier plots in LIHC (G) and Cohort 1 (I). (J) Relative MVP expression in 28 patients with HCC treated with anti-PD-1/PD-L1. (K) Percentage of patients with HCC with PR or SD/PD after anti-PD-1/PD-L1 treatment in the low-MVP or high-MVP expression groups. *p<0.05, **p<0.01, ***p<0.001. p<0.05 was considered statistically significant. ChIP-seq, chromatin immunoprecipitation followed by sequencing; FDR, false discovery rate; HCC, hepatocellular carcinoma; ICIs, immune checkpoint inhibitors; KEGG, kyoto encyclopedia of genes and genomes; LDHi, lactate dehydrogenase inhibitor; LIHC,Liver hepatocellular carcinoma; MVP, major vault protein; PD, progressive disease; PD-1, programmed cell death protein-1; PD-L1, programmed cell death-ligand 1; PR, partial response; RNA-seq, RNA sequencing; SD, stable disease.

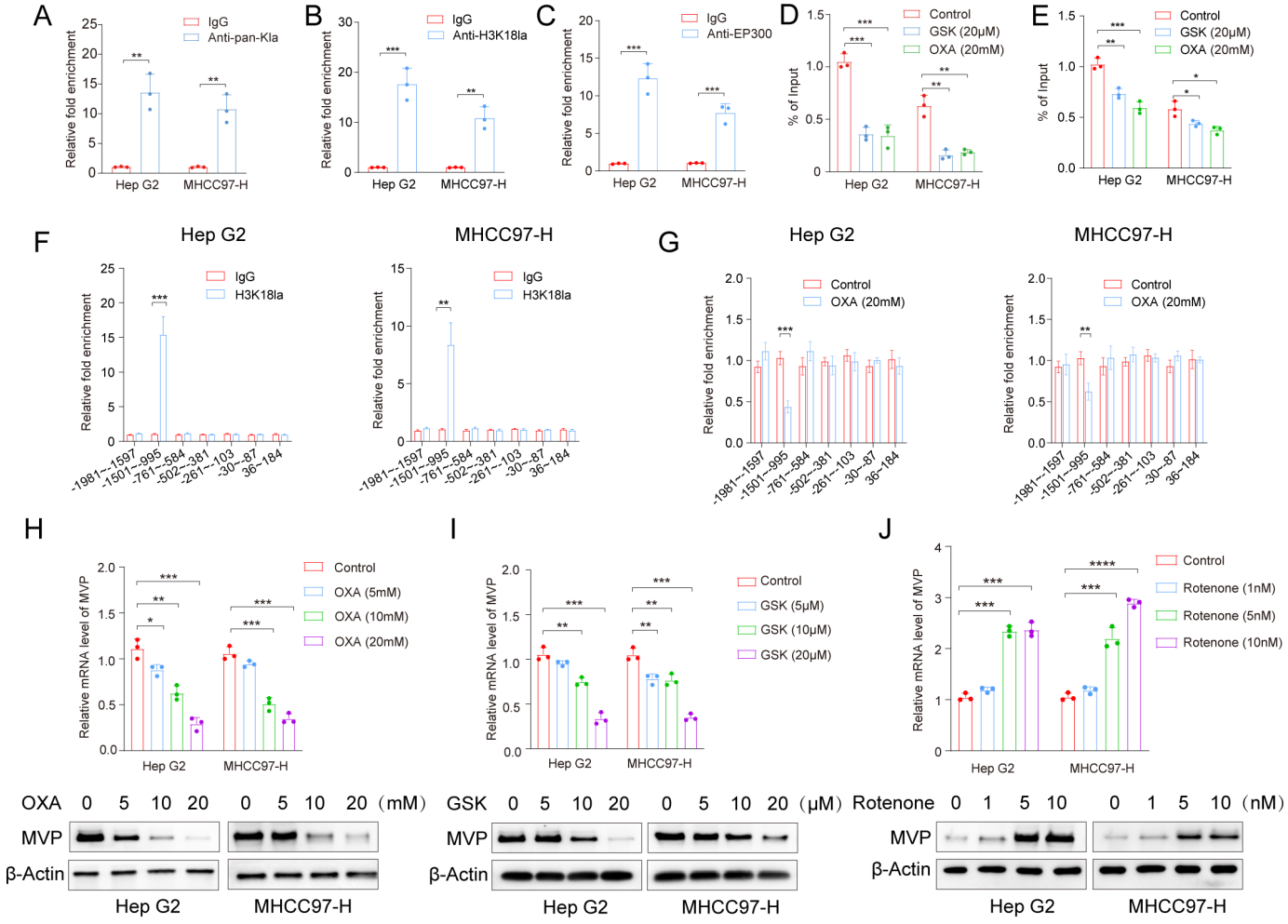

Figure 4 H3K18la activates transcription of MVP. (A–C) DNA fragments from Hep G2 and MHCC97-H cells were immunoprecipitated with pan-lactylation (A), H3K18la (B) and EP300 (C) antibodies and then analyzed by qPCR. (D–E) ChIP-qPCR analysis of H3K18la (D) and EP300 (E) enrichment at the promoter of MVP in Hep G2 and MHCC97-H cells after treatment with LDHi. (F) ChIP-qPCR assay of H3K18la enrichment at the indicated region of the MVP promoter in Hep G2 and MHCC97-H cells. (G) ChIP-qPCR analysis of H3K18la enrichment at the indicated region of the MVP promoter in Hep G2 and MHCC97-H cells after treatment with LDHi. (H–J) Relative expression of MVP was detected in Hep G2 and MHCC97-H cells after treatment with different concentrations of oxamate (H), GSK2937808A (I) and rotenone (J). *p<0.05, **p<0.01, ***p<0.001,****p<0.0001. p<0.05 was considered statistically significant. ChIP, chromatin immunoprecipitation; LDHi, lactate dehydrogenase inhibitor; MVP, major vault protein; mRNA, messenger RNA; qPCR, quantitative PCR.

MVP attenuates CD8$^+$ T cell-mediated antitumor immunity in HCC

Although MVP is known to contribute to tumor progression and therapeutic resistance, its role in the TME remains poorly defined. We generated knockout cell lines of MVP in Hep G2 and Hepa 1–6 cells (figure 5A). To assess the impact of MVP on T-cell function, an in vitro T cell-mediated killing assay was performed, in which HCC cells were co-cultured with activated T cells at a 1:5 ratio. The results showed that T cells co-cultured with MVP-knockout HCC cells exhibited enhanced cytotoxicity, resulting in increased tumor cell apoptosis (figure 5B–E). Conversely, MVP-overexpressing HCC cells displayed resistance to T cell-mediated killing, highlighting MVP's potential role in suppressing antitumor immunity (figure 5D,E). Given our previous findings that lactate-induced lactylation regulated immune responses through CD8$^+$ T cells, we proceeded to explore whether the immunosuppressive effects of MVP were mediated through this subset. Hepa 1–6 cells carrying luciferase reporters were orthotopically inoculated into C57BL/6 mice, with or without anti-CD8 monoclonal antibody administration. Compared with controls, MVP depletion significantly inhibited tumor growth and prolonged the survival of tumor-bearing mice (figure 5F–H). As anticipated, MVP knockout increased CD8$^+$ T-cell infiltration in the TME (figure 5I). Moreover, MVP-deficient HCC increased the proportion of IFN-γ$^+$, GzmB$^+$, TNF-α$^+$ and perforin$^+$CD8$^+$ T-cell subsets, indicating enhanced cytotoxic T-cell function (figure 5J–M). Correspondingly, TNF-α and IFN-γ concentrations were elevated in the TME of MVP-knockout mice (figure 5N). However, in CD8$^+$ T cell-depleted mice, MVP knockout failed to affect tumor burden or survival, and CD8$^+$ T-cell subset proportions remained unchanged, confirming

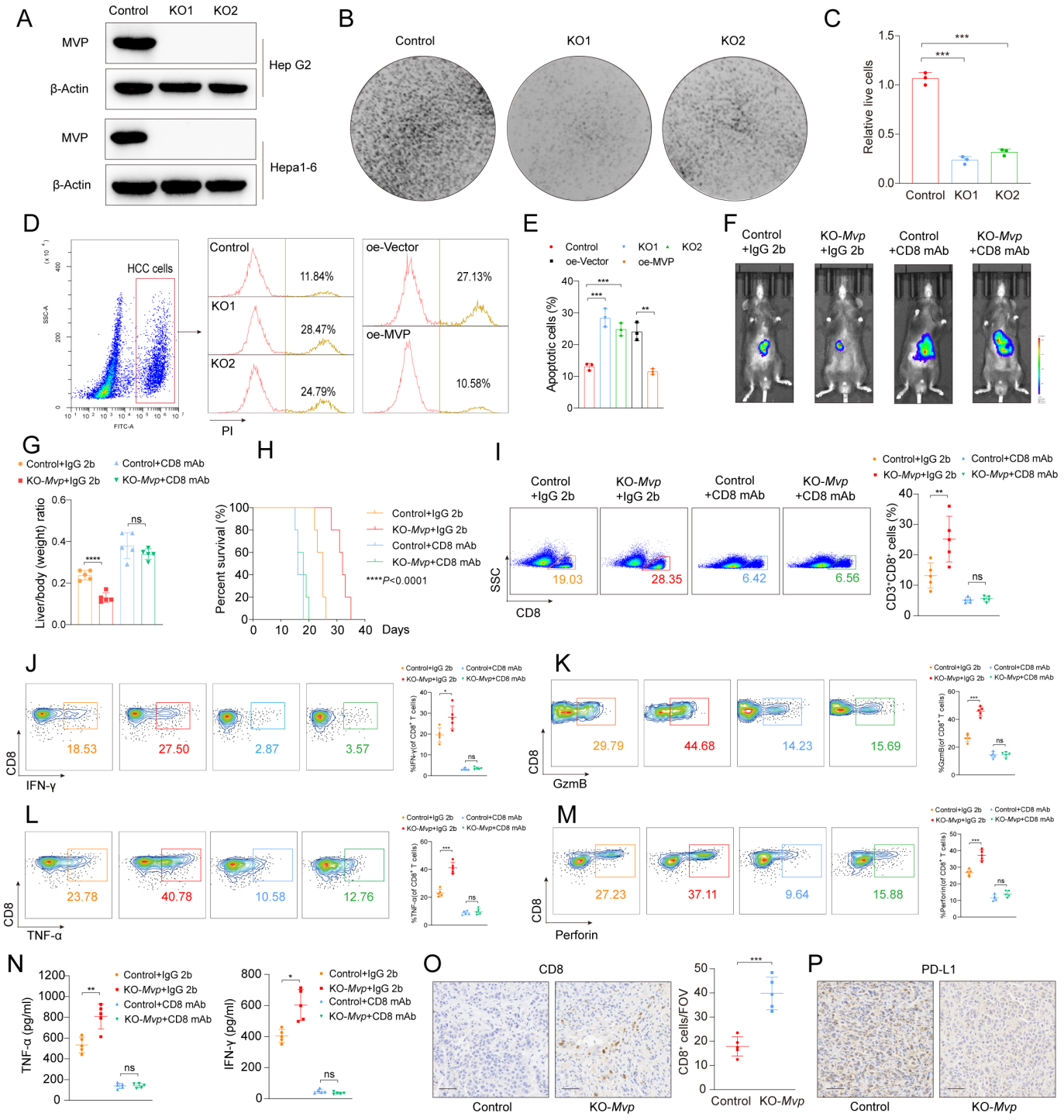

Figure 5 MVP attenuates CD8$^+$ T cell-mediated antitumor immunity in HCC. (A) Western blot verified almost disappeared MVP expression in MVP-KO HCC cells. (B–C) Results of the T cell-mediated cancer cell-killing assay. Control or MVP-knockout HCC cells were co-cultured with activated T cells for 48 hours and stained with crystal violet. The ratio of tumor cells to T cells was 1:5. Representative images of live cells were shown (B) and further quantified (C). (D–E) Percentage of apoptotic HCC cells in each group after co-cultured with activated T cells for 48 hours and stained with PI, analyzed by flow cytometry. The ratio of tumor cells to T cells was 1:5. (F) Representative fluorescence images of mice in each group. (G) Weight of orthotopic tumor in each group (n=5). (H) Survival of mice in each group assessed by Kaplan-Meier survival curves with log-rank test (n=5). (I) Proportion of intratumor CD8$^+$ T cells was analyzed by flow cytometry. (J–M) Flow cytometric analysis of the IFN-γ$^+$ (J), GzmB$^+$ (K), TNF-α$^+$ (L), and perforin$^+$ (M) CD8$^+$ TILs from control and MVP-KO orthotopic models. (N) TNF-α and IFN-γ concentrations in the control and MVP-KO orthotopic models. (O–P) Representative images of tumor-infiltrating CD8$^+$ lymphocytes (O) and PD-L1 expression (P) in the control and MVP-KO orthotopic models analyzed by immunohistochemistry (scale bar: 100 µm). *p<0.05, **p<0.01, ***p<0.001, ****p<0.0001. p<0.05 was considered statistically significant. FOV, field of view; GzmB, granzyme B; HCC, hepatocellular carcinoma; IFN, interferon; KO, knock out; MVP, major vault protein; PD-L1, programmed cell death-ligand 1; TILs, tumor infiltrating lymphocytes; TNF, tumor necrosis factor.

that MVP exerts its immunosuppressive effect primarily by inhibiting $CD8^+$ T-cell activity (figure 5F–M). These findings were further corroborated by IHC analysis showing increased $CD8^+$ T-cell infiltration in the MVP-deficient group (figure 5O). Given the critical role of immune checkpoint molecules in regulating T-cell function, we next assessed their expression following MVP depletion. IHC revealed a significant downregulation of PD-L1 in the TME of MVP-deficient tumors, suggesting that MVP may influence T-cell activity by modulating PD-L1 expression (figure 5P).

MVP inhibits ubiquitination-mediated proteasomal degradation of PD-L1

In order to elucidate the mechanisms by which MVP affects T-cell function, we evaluated PD-L1 expression in HCC cells with either MVP knockout or overexpression. MVP depletion reduced the expression of PD-L1 in HCC cells, whereas overexpression of MVP led to the upregulation of PD-L1 (figure 6A,B). Besides, a positive correlation between MVP and PD-L1 protein levels was observed in HCC samples, analyzed by western blot and IHC (online supplemental figure 5A and B). Notably, CD274 mRNA levels remained unchanged after MVP modulation, indicating that MVP regulated PD-L1 expression at the post-transcriptional level (figure 6C). Treatment with the proteasome inhibitor MG132 rescued PD-L1 protein levels in MVP-deficient cells, implying that MVP modulated PD-L1 levels via ubiquitination-mediated proteasomal degradation (figure 6D). Supporting this, PD-L1 protein displayed a shorter half-life in MVP-knock out HCC cells compared with controls, which could be rescued by MG132 treatment (figure 6E,F). Conversely, MVP overexpression extended the half-life of PD-L1 (figure 6G). Elevated PD-L1 ubiquitination was detected in MVP-depleted cells (figure 6H). Additionally, loss of MVP abolished lactate-induced PD-L1 upregulation, implicating MVP as a mediator of lactate-driven PD-L1 stabilization (online supplemental figure 5C). In conclusion, our data confirmed that lactylation-induced MVP upregulation inhibited the ubiquitination-mediated proteasomal degradation of PD-L1.

MVP inhibits ubiquitination-mediated proteasomal degradation of PD-L1 through competitively binding with β-TrCP

To elucidate the mechanism underlying MVP-mediated stabilization of PD-L1, we conducted co-immunoprecipitation (co-IP) experiments followed by mass spectrometry. After excluding non-specific IgG-binding proteins, 76 proteins were identified to interact with MVP. Among these, β-TrCP—a known E3 ubiquitin ligase involved in PD-L1 degradation—was of particular interest[25 26] (figure 7A). The physical interaction between MVP and β-TrCP proteins was further confirmed by co-IP (figure 7B,C). Immunofluorescence staining demonstrated cytoplasmic co-localization of endogenously expressed β-TrCP and MVP (figure 7D). Previous structural studies have shown that each MVP monomer folds into 12 domains—comprising 9 structural repeats, a shoulder domain, a cap-helix domain, and a cap-ring domain. Interactions between the 42-turn-long cap-helix domains are key to stabilizing the vault particle.[27] To determine the β-TrCP-binding domain within MVP, we employed computational modeling of the β-TrCP–MVP interaction. β-TrCP structure extracted from the Protein Data Bank (PDB 6TTU) was docked onto an MVP chain derived from the vault crystal structure (PDB 4HL8) using a blind docking method. The results showed that the MVP–β-TrCP complex predominantly interacts through the cap-helix domain of MVP (Ala^{622}-Leu^{802}) (online supplemental figure 6A). Co-IP assays further confirmed that deletion of the residues Ala^{622}-Lys^{674} within MVP sequence markedly reduced MVP–β-TrCP binding (online supplemental figure 6B and C). Notably, PD-L1 harbors a conserved β-TrCP recognition motif (D/LSGXXS), suggesting its involvement in MVP-mediated PD-L1 degradation (figure 7E). To further explore this, we generated a PD-L1 S176A mutant construct and assessed the degradation kinetics of Flag-PD-L1-WT and Flag-PD-L1-S176A using cycloheximide chase assays. As shown in the results, the S176A mutation significantly extended the half-life of the PD-L1 protein (figure 7F,G). Ubiquitination conjugation assay confirmed that the S176A variant remarkably inhibited the ubiquitination of PD-L1 relative to the wild-type (figure 7H). Moreover, mutation of PD-L1 S176A also weakened its binding with β-TrCP (figure 7I). Further analyses revealed that MVP overexpression did not affect β-TrCP mRNA or protein levels (figure 7J). However, the overexpression of MVP rescued the inhibitory effect of β-TrCP on PD-L1 (figure 7K,L). Conversely, β-TrCP knockout rescued the decline of PD-L1 caused by MVP depletion, indicating that MVP regulated PD-L1 expression through β-TrCP-mediated proteasomal degradation (figure 7M). Competitive binding assays showed that MVP overexpression hinders the binding of β-TrCP to PD-L1 (figure 7N,O). Moreover, MVP rescued the increased ubiquitination level of PD-L1 caused by β-TrCP overexpression (figure 7P). To further validate the role of Ala^{622}–Lys^{674} region of MVP in regulating PD-L1 stability, we performed a protein stability assay of PD-L1 after overexpressing truncated MVP removing amino acids 622–674. Our results confirmed that the wild-type MVP, but not the truncated MVP, rescued the shortened half-life of PD-L1 caused by MVP knockout (online supplemental figure 6D and E). Besides, truncated MVP also failed to rescue the increased ubiquitination of PD-L1 in MVP-KO HCC cells, indicating Ala^{622}–Lys^{674} region is necessary for MVP function in PD-L1 regulatory mechanism (online supplemental figure 6F).In summary, our findings demonstrated that MVP stabilizes PD-L1 by competitively inhibiting β-TrCP-mediated degradation.

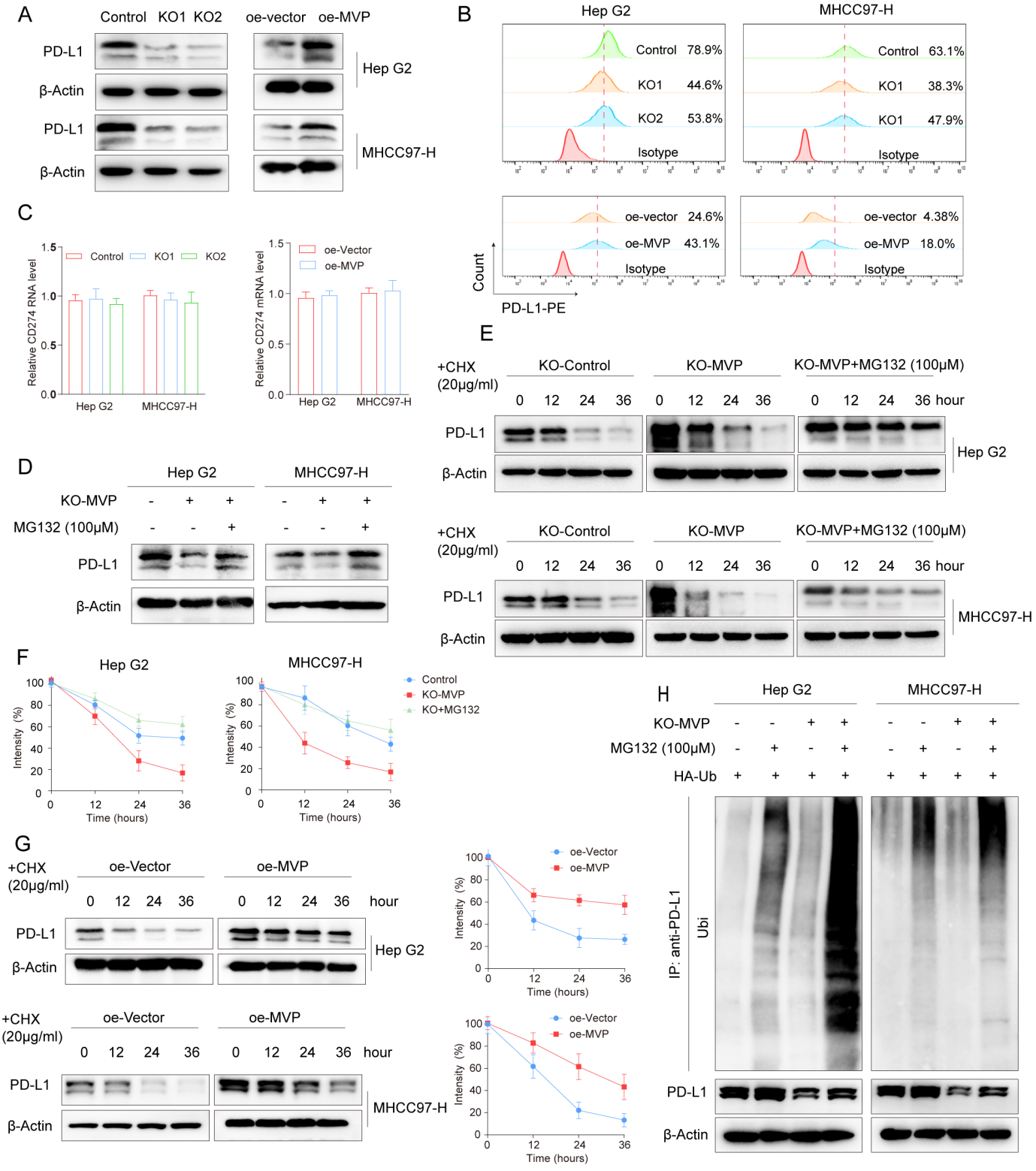

Figure 6 MVP inhibits ubiquitination-mediated proteasomal degradation of PD-L1. (A–B) Western blot (A) and flow cytometric analyses (B) of PD-L1 expression in HCC cell lines after MVP knockout or overexpression. (C) mRNA level of CD274 was assessed through qRT-PCR in HCC cell lines after MVP knockout or overexpression. (D) Western blot analysis of PD-L1 expression in MVP knockout HCC cells after treatment with MG132 (100 μM, 24 hours). (E) Stability analysis of the PD-L1 protein in control and MVP-KO HCC cells treated with CHX (20 μg/mL). (F) Statistical quantitation of the PD-L1 protein intensity in control and MVP-KO HCC cells treatment with CHX (20 μg/mL). (G) Stability analysis of PD-L1 protein in control and MVP overexpression HCC cells treated with CHX (20 μg/mL). (H) Ubiquitination assay of PD-L1 in MVP knockout cells after treatment with MG132 (100 μM, 24 hours). CHX, cycloheximide; HCC, hepatocellular carcinoma; KO, knock out; MVP, major vault protein; mRNA, messenger RNA; PD-L1, programmed cell death-ligand 1; qRT-PCR, quantitative reverse-transcription polymerase chain reaction.

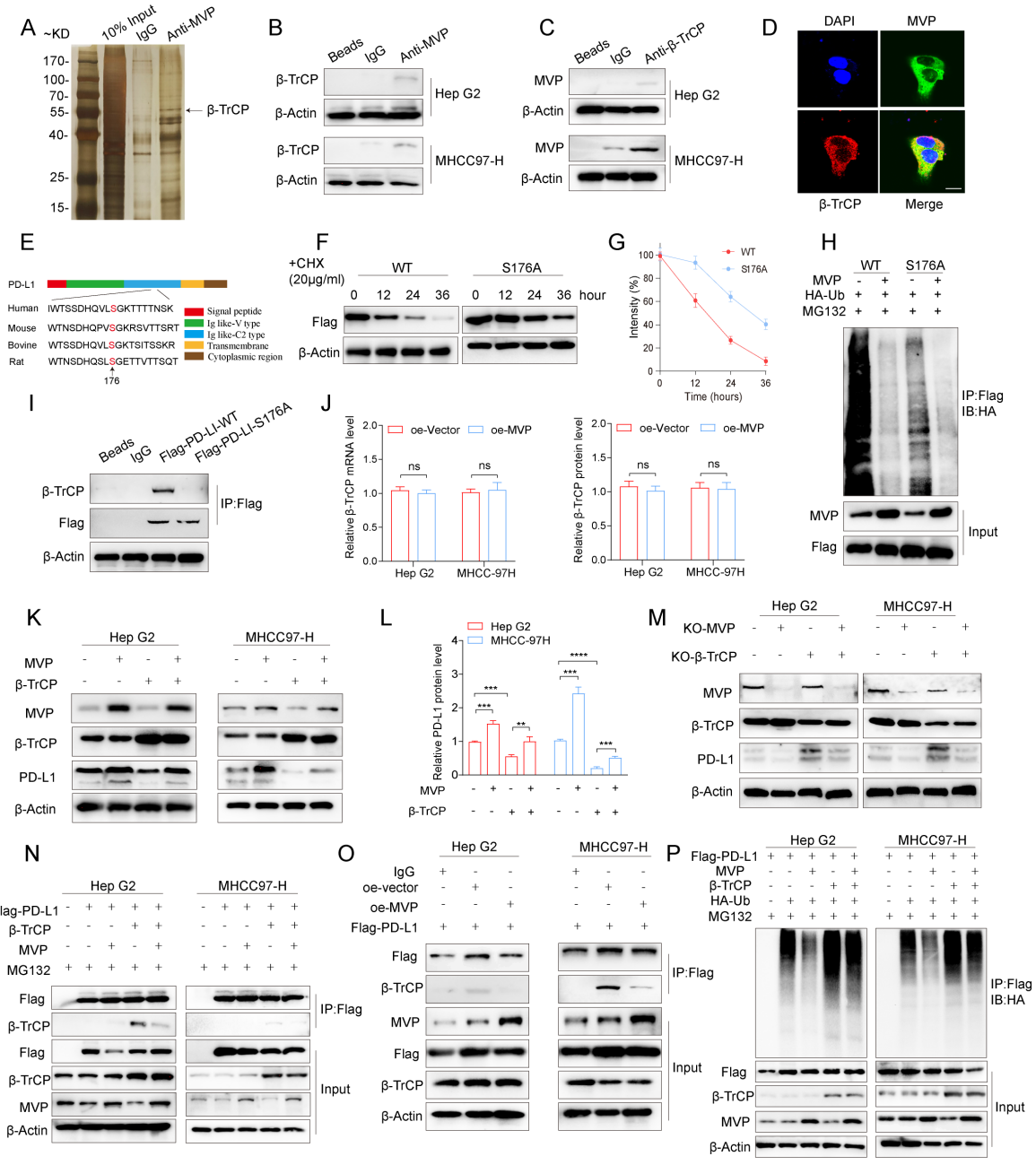

Figure 7 MVP inhibits ubiquitination-mediated proteasomal degradation of PD-L1 through competitively binding with β-TrCP. (A) Co-IP assay conducted using anti-MVP. Samples were separated by silver staining followed by mass spectroscopy. The black arrow indicated β-TrCP. (B–C) Interaction between MVP and β-TrCP was confirmed by co-IP assay followed by western blot. (D) Immunofluorescence image of endogenous MVP and β-TrCP proteins in Hep G2 cells (scale bar: 20 μm). (E) Sequence alignment of PD-L1 protein in mammalian species. Amino acid residue at S176 is conserved across different mammalian species. (F) Stability analysis of wild-type flag-PD-L1 protein and flag-PD-L1 mutants (S176A) after treatment with CHX (20 μg/mL). (G) Statistical quantitation of the degradation rate of wild-type PD-L1 and PD-L1 mutants (S176A) after treatment with CHX (20 μg/mL). (H) In vitro ubiquitin conjugation assay comparing the extent of ubiquitination of wild-type PD-L1 and PD-L1 mutants (S176A) with or without MVP overexpression in HEK-293T cells. (I) Interaction between β-TrCP and wild-type flag-PD-L1 protein or flag-PD-L1 mutants (S176A) was confirmed by co-IP assay followed by western blot. (J) Expression level of β-TrCP messenger RNA and protein in hepatocellular carcinoma cell lines after MVP overexpression. (K) Western blot analysis showing the effect of MVP and/or β-TrCP ectopic overexpression on PD-L1 expression in Hep G2 and MHCC97-H cells. (L) Statistical quantitation of PD-L1 protein after MVP and/or β-TrCP ectopic overexpression in Hep G2 and MHCC97-H cells. (M) Western blot analysis showing the effect of MVP and/or β-TrCP knockout on PD-L1 expression in Hep G2 and MHCC97-H cells. (N) Co-IP assay showing the competition of MVP with PD-L1 for binding to β-TrCP. (O) Co-IP assay showed β-TrCP protein level precipitated by PD-L1 after ectopic MVP overexpression. (P) In vitro ubiquitin conjugation assay showing reduced ubiquitination of PD-L1 when MVP competed with PD-L1 for binding to β-TrCP. **p<0.01, ***p<0.001, ****p<0.0001. p<0.05 was considered statistically significant. β-TrCP, β-transducin repeat-containing protein; CHX, cycloheximide; co-IP, co-immunoprecipitation; DAPI, 4',6-diamidino-2-phenylindole; KD, kiloDalton; MVP, major vault protein; PD-L1, programmed cell death-ligand 1.

Inhibition of lactylation enhances the antitumor effects of anti-PD-1 immunotherapy in HCC

Given that MVP regulated the stability of PD-L1 protein, we hypothesized that targeting MVP could enhance the therapeutic efficacy of anti-PD-1 immunotherapy. As expected, MVP knockdown combined with anti-PD-1 treatment significantly enhanced T cell-mediated cytotoxicity in vitro compared with anti-PD-1 monotherapy, leading to increased apoptosis of HCC cells in the co-culture system (online supplemental figure 7A-D). To further evaluate this strategy in vivo, we established an orthotopic HCC model by injecting luciferase-labeled Hepa 1–6 cells into the livers of C57BL/6 mice. The mice were then treated with LDHi, anti-PD-1 antibody, or their combination, according to the experimental design (figure 8A). Tumors in the combination therapy group had a dramatically less

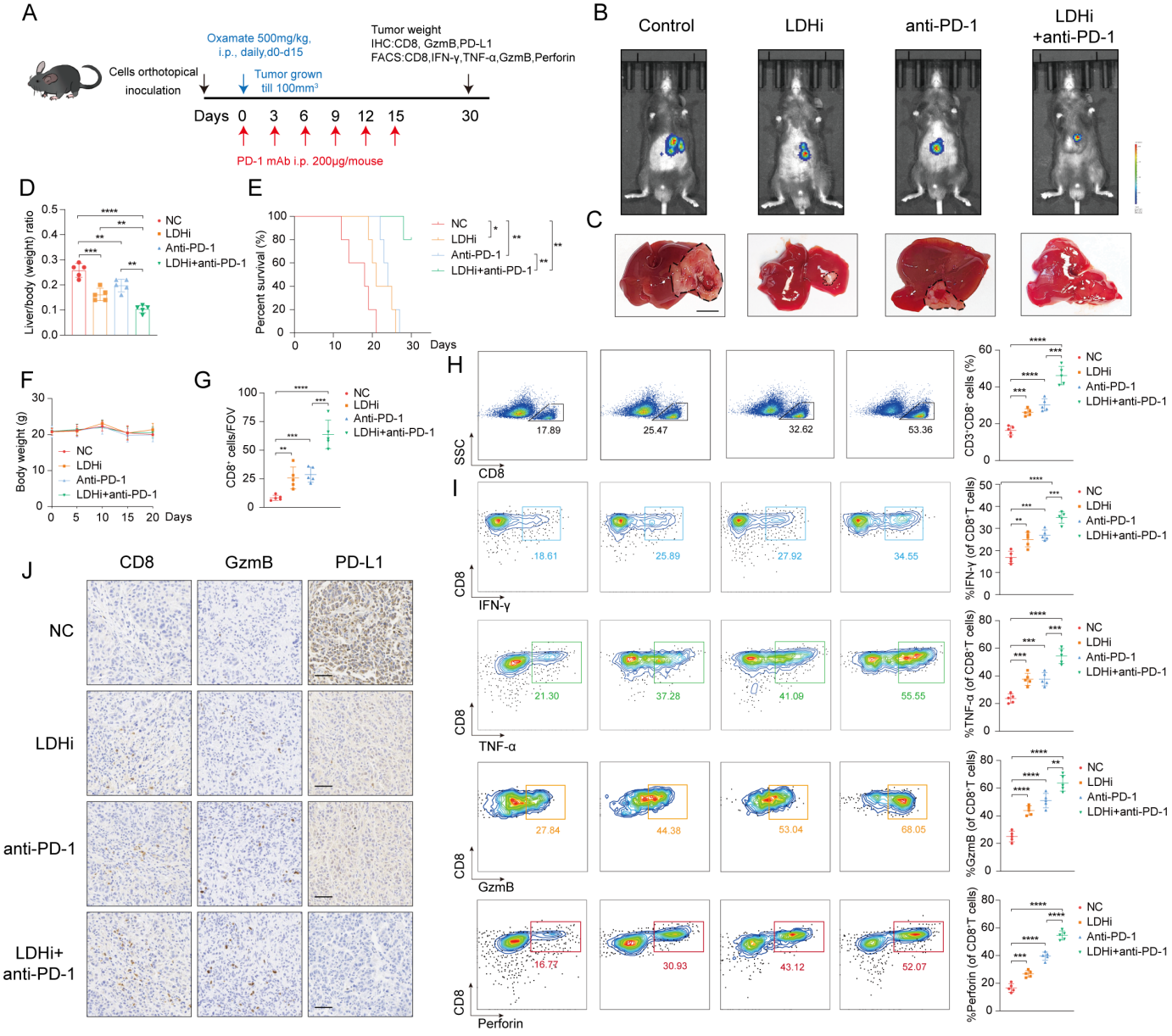

Figure 8 Inhibition of lactylation enhances the antitumor effects of anti-PD-1 immunotherapy in HCC. (A) Schematic diagram of animal experiments. (B) Representative fluorescence images of orthotopic HCC models in each group. (C) Representative images of tumors after dissection (scale bars: 5 mm). (D) Weight of orthotopic tumor in each group (n=5). (E) Survival of mice in each group assessed by Kaplan-Meier survival curves using the log-rank test (n=5). (F) Body weight of mice among the groups (n=5). (G–H) Intratumor $CD8^+$ T cells were analyzed by IHC staining (G) and flow cytometry (H) (n=5). (I) Flow cytometric analysis of the IFN-γ^+, TNF-α^+, $GzmB^+$ and perforin$^+$ $CD8^+$ TILs in the orthotopic tumor in each group (n=5). (J) Representative IHC staining images of CD8, granzyme B, and PD-L1 from the four groups (scale bars: 100 μm). *p<0.05, **p<0.01, ***p<0.001, ****p<0.0001. p<0.05 was considered statistically significant. FACS, fluorescence-activated cell sorting; GzmB, granzyme B; HCC, hepatocellular carcinoma; IFN, interferon; IHC, immunohistochemistry; i.p., intraperitoneal injection; LDHi, lactate dehydrogenase inhibitor; mAb, monoclonal antibody; NC, negative control; PD-1, programmed cell death protein-1; PD-L1, programmed cell death-ligand 1; TNF, tumor necrosis factor.

vigorous fluorescence intensity than the monotherapy groups, with smaller tumor volumes and lighter tumor weights (figure 8B–D). The mice that received combination treatment also displayed better survival than those in the other groups (figure 8E). No notable weight loss was detected with the combination treatment (figure 8F). Flow cytometric analysis illustrated a notable increase of intratumoral $CD8^+$ T-cell infiltration following the combination therapy, alongside elevated expression of effector molecules including IFN-γ, TNF-α, GzmB, and perforin, indicating enhanced cytotoxic T-cell activity (figure 8H,I). The increase in the quantity and activation of $CD8^+$ T cells was further validated by IHC (figure 8G and J). We also evaluated the side effects of combination therapy. Blood samples were collected on day 15 after treatment for hematological and biochemical profiling, including liver function (alanine aminotransferase (ALT), aspartate aminotransferase (AST), total bilirubin (TBIL)) and renal function (blood urea nitrogen (BUN), creatinine (CREA)) markers. As our results showed, no statistically significant differences were observed in liver enzymes, kidney function and hematologic toxicity between two groups, supporting the safety of the combination regimen (online supplemental table 2). To further assess possible systemic toxicity, the major organs were harvested for histological analysis through H&E staining. As shown in the result, no significant pathological changes were found in the heart, brain, liver, lung, spleen, or kidney tissues by histological examination, indicating no notable toxicity in the combination group (online supplemental figure 8A). Overall, our results demonstrated that co-targeting lactylation and PD-1 enhanced the immunotherapeutic antitumor response with acceptable side effects in HCC.

DISCUSSION

Immunotherapy represents a major breakthrough in the treatment of advanced HCC, improving both OS and quality of life. Nonetheless, the modest response rates and frequent development of resistance to ICIs impede its efficacy and clinical applicability. A major challenge lies in the metabolically hostile TME, which is characterized by acidity, hypoxia, and ischemia. The immunoregulatory role of lactate has been increasingly recognized, linking metabolic rearrangements firmly to the tumor immunity. Persistently elevated lactate concentrations contribute to the formation of an immunosuppressive TME. While previous research has primarily focused on lactate's role as an energy substrate and signaling molecule in immune regulation, recent studies have uncovered its involvement in epigenetic modulation via histone lactylation, offering new perspectives on lactate-driven immunosuppression. Our research has demonstrated elevated levels of histone lactylation in patients with HCC resistant to ICIs, correlating with poor survival outcomes. Patients who later developed PD displayed higher lactylation levels than those who achieved SD, suggesting an inverse relationship between histone lactylation and immunotherapy efficacy. Furthermore, MVP was identified as a downstream effector of H3K18la, with increased expression in patients who developed SD and PD following PD-1/PD-L1 treatment. These results suggest that MVP may serve as a potential biomarker for predicting the efficacy of tumor immunotherapy. Mechanistically, H3K18la-driven upregulation of MVP attenuates $CD8^+$ T cell-mediated antitumor immunity by inhibiting the ubiquitination-mediated proteasomal degradation of PD-L1.

Post-translational modifications of histones—such as methylation, acetylation, ubiquitination, phosphorylation, and other less common modifications—play important roles in DNA-related processes including transcription, replication, and repair.[28] These modifications maintain the balance between transcriptional activation and repression of genes, thus governing gene expression and regulating biological outcomes. Disruption of this balance leads to dysregulation of chromatin structure and gene expression patterns, contributing to malignant transformation and therapeutic resistance. Lactylation, a recently identified post-translational modification, has emerged as a key regulator of drug resistance in cancer. For example, lactylation of NBS1 promotes homologous recombination-mediated DNA repair and contributes to chemoresistance in cancer.[29] In colorectal cancer, patients resistant to bevacizumab exhibit elevated histone lactylation, while pharmacologic inhibition of this modification suppresses tumorigenesis and progression.[30] H3K18la-driven transcription factors YBX1 and YY1 promote cisplatin resistance in bladder cancer.[31] In this study, we demonstrated that elevated histone lactylation is associated with poor clinical outcomes in patients with HCC treated with ICIs. Inhibition of lactylation enhanced $CD8^+$ T-cell infiltration and augmented antitumor activity in TME. Notably, this inhibition also led to a decrease in natural killer (NK) cell infiltration, which may potentially hamper the antitumor immune responses. However, tumor metastases were not more pronounced following treatment with LDHi, suggesting that the decrease in NK cells was insufficient to drive distant dissemination. This could be attributed to LDHi-induced remodeling of the TME toward a cytotoxic, rather than immunosuppressive phenotype. To explore the mechanisms underlying this observation, we re-analyzed RNA-seq data from human HCC cell lines treated with LDHi. We identified reduced expression of several chemokines involved in localization of NK cells, including CCL2, CCL5, and CCL7. The observed changes in the tumor's chemokine profile induced by LDHi may be partly responsible for diminished NK cell infiltration in the TME. However, given that current evidence is limited to in vitro analyses, further in vivo validation is warranted. Besides, we also observed a mild but not statistically significant increase of monocyte/macrophage subsets after oxamate treatment. Collectively, our findings provide a novel strategy of combining lactylation inhibitors with ICIs to improve the clinical efficacy of immunotherapy in HCC.

Multiomics analyses have identified MVP as a downstream effector of histone lactylation. MVP has attracted a great deal of attention from researchers in recent years due

to its multifaceted roles in cancer biology.[32–35] Beyond its established function in mediating drug resistance, MVP also participates in immune regulation and surveillance. It acts as a molecular sentinel in inflammation-driven processes, such as TRAIL-mediated apoptotic signaling.[36] In prostate cancer, a study involving 119 patients reported a positive correlation between MVP and the immune checkpoint molecule B7-H3, highlighting MVP's key role in cancer immunoregulation.[37] Additionally, MVP serves as a scaffold for multimolecular complexes and regulates exosomal cargo loading. For instance, MVP facilitates the incorporation of miR-193a into exosomes, promoting colon cancer growth and metastasis.[38 39] In our study, we revealed that H3K18la upregulates MVP, which in turn attenuates $CD8^+$ T cell-mediated antitumor immunity by stabilizing PD-L1. Mechanistically, MVP inhibits the ubiquitin-mediated proteasomal degradation of PD-L1 by competitively binding to the E3 ubiquitin ligase β-TrCP. In light of these findings, we propose MVP as a pivotal therapeutic target within the context of HCC management, which cannot only partly reverse the immunosuppressive microenvironment, but can also overcome the resistance of ICIs. Suloctidil and tetradioxin are identified as potential MVP-specific targeted agents with binding affinities and configurations based on drug databases and structural analysis.[40] More explorations are needed to confirm their pharmacological effects. Dual targeting of MVP and immune checkpoints may offer a promising approach to augment antitumor immune responses in HCC.

The limited understanding of lactylation has hindered the development of specific inhibitors. Currently, lactylation is typically suppressed by inhibiting glycolytic enzymes, particularly LDH, which catalyzes the conversion of pyruvate to lactate in aerobic glycolysis. Extensive research implicates LDH in cancer progression via tumor glycolysis and lactate shuttling, influencing energy metabolism, angiogenesis, cell survival, and therapeutic resistance. LDHA, predominantly expresses in skeletal muscle and liver, exhibits elevated activity in patients with HCC, making it a promising therapeutic target. Although several LDHA inhibitors have shown efficacy in preclinical models, none have been approved for clinical use yet.[41] The principal challenge lies in potential systemic toxicity due to non-specific protein expression when LDHA inhibitors are used as monotherapy. Therefore, combination strategies are urgently needed to optimize therapeutic efficacy while minimizing adverse effects. Previous studies have indicated that combining LDHis (eg, oxamate) with pembrolizumab enhances $CD8^+$ T-cell infiltration and boosts the therapeutic effect in non-small cell lung cancer.[42] Consistent with these findings, our data confirm that LDH inhibition enhances the antitumor effects of anti-PD-1 therapy in HCC, offering a favorable risk-benefit profile with limited severe side effects. This finding sheds new light on the potential of immunotherapies incorporating lactylation inhibition.

In conclusion, our study reveals that histone lactylation-induced upregulation of MVP stabilizes PD-L1 protein by preventing β-TrCP-mediated proteasomal degradation. We demonstrate a novel mechanism of immune escape mediated by lactate, providing an important entry point for examining metabolism-induced epigenetic landscape and its relationship with immune microenvironment. Moreover, combining lactylation inhibitors with anti-PD-1/PD-L1 therapies enhances the efficacy and addresses ICIs resistance in HCC. This approach avoids the non-specific cytotoxicity commonly associated with high doses of LDHi, thus providing a potent clinical option for HCC treatment. Consequently, apart from inhibiting glycolysis, LDHi can be regarded as a reversal agent with extraordinary potential for overcoming ICIs resistance in HCC.

There were several limitations in this research. First, the sample sizes and the follow-up time of the ICIs-treated cohort were limited, warranting further validation in larger and longitudinally monitored populations. Second, pharmacological targeting of lactylation in vivo remains challenging due to the lack of specific inhibitors. Perturbations to metabolic homeostasis induced by LDHi require more comprehensive evaluations. Third, a more detailed characterization of the tumor immune microenvironment (TIME) before and after treatments, and the expression profiles of immune checkpoint molecules across diverse immune cell subsets is needed to elucidate mechanistic insights more fully.

Author affiliations
[1]Department of Oncology, Third Affiliated Hospital of Soochow University, Changzhou, Jiangsu, China
[2]Department of Urology, Third Affiliated Hospital of Soochow University, Changzhou, Jiangsu, China
[3]Sun Yat-sen University Cancer Center, Guangzhou, China
[4]Department of Colorectal Surgery, Hunan Cancer Hospital, Changsha, Hunan, China
[5]Department of Tumor Biological Treatment, Third Affiliated Hospital of Soochow University, Changzhou, Jiangsu, China
[6]Institute of Cell Therapy, Soochow University, Suzhou, Jiangsu, China

Contributors The author SL and WL designed the study. SL and YP conducted the molecular biological experiments. XB performed the bioinformatics analyses. RS and QW contributed to the procedures of animal experiments. JX and CheW contributed to the writing of article. JW and WH contributed to proofreading the article. ChaW and JJ contributed to the platform and the funding support. JJ is the guarantor for contributorship statement.

Funding This work was supported by National Natural Science Foundation Program of China (82403938, 82303164, 81972869, 32270955), Natural Science Research of Jiangsu Higher Education Institutions of China (23KJB320018), China Postdoctoral Science Foundation (2023M730374, 2024M750279), Clinical Frontier Technology Project of the Jiangsu Key Research and Development (BE2022719), Leading Innovative Talents of Changzhou (CQ20220114, CQ20220129), Natural Science Foundation of Jiangsu Province (BK20240342), and Provincial-level Talent Program for National Center of Technology Innovation for Biopharmaceuticals (NCTIB2024JS0101).

Competing interests No, there are no competing interests.

Patient consent for publication Not applicable.

Ethics approval Ethics Committee of the Third Affiliated Hospital of Soochow University (Ethics approval number: (2023)KE-198). Written informed consent was obtained from each patient before participation in the study.

Provenance and peer review Not commissioned; internally peer reviewed.

Data availability statement Data are available upon reasonable request. All data associated with this study are presented in the paper or the Supplementary Data. The materials supporting the findings of this study are available from the corresponding author upon reasonable request.

ORCID iDs
Shuang Liu http://orcid.org/0000-0002-6647-6197
Yihui Pan http://orcid.org/0009-0008-3221-953X
Wenjian Liu http://orcid.org/0009-0005-6388-7758
Xiaoyun Bu http://orcid.org/0000-0001-6455-1774
Ruonan Shao http://orcid.org/0000-0002-5566-1848
Jingting Jiang http://orcid.org/0000-0002-3128-9762

REFERENCES

1 Sung H, Ferlay J, Siegel RL, *et al*. Global Cancer Statistics 2020: GLOBOCAN Estimates of Incidence and Mortality Worldwide for 36 Cancers in 185 Countries. *CA Cancer J Clin* 2021;71:209–49.
2 Finn RS, Qin S, Ikeda M, *et al*. Atezolizumab plus Bevacizumab in Unresectable Hepatocellular Carcinoma. *N Engl J Med* 2020;382:1894–905.
3 Llovet JM, Kelley RK, Villanueva A, *et al*. Hepatocellular carcinoma. *Nat Rev Dis Primers* 2021;7:6.
4 Llovet JM, Castet F, Heikenwalder M, *et al*. Immunotherapies for hepatocellular carcinoma. *Nat Rev Clin Oncol* 2022;19:151–72.
5 Hanahan D. Hallmarks of Cancer: New Dimensions. *Cancer Discov* 2022;12:31–46.
6 Pavlova NN, Zhu J, Thompson CB. The hallmarks of cancer metabolism: Still emerging. *Cell Metab* 2022;34:355–77.
7 Certo M, Tsai C-H, Pucino V, *et al*. Lactate modulation of immune responses in inflammatory versus tumour microenvironments. *Nat Rev Immunol* 2021;21:151–61.
8 Wang Z-H, Peng W-B, Zhang P, *et al*. Lactate in the tumour microenvironment: From immune modulation to therapy. *EBioMedicine* 2021;73:103627.
9 Zhang D, Tang Z, Huang H, *et al*. Metabolic regulation of gene expression by histone lactylation. *Nature New Biol* 2019;574:575–80.
10 Chen A-N, Luo Y, Yang Y-H, *et al*. Lactylation, a Novel Metabolic Reprogramming Code: Current Status and Prospects. *Front Immunol* 2021;12:688910.
11 Moreno-Yruela C, Zhang D, Wei W, *et al*. Class I histone deacetylases (HDAC1-3) are histone lysine delactylases. *Sci Adv* 2022;8:eabi6696.
12 Yang Z, Yan C, Ma J, *et al*. Lactylome analysis suggests lactylation-dependent mechanisms of metabolic adaptation in hepatocellular carcinoma. *Nat Metab* 2023;5:61–79.
13 Jin J, Bai L, Wang D, *et al*. SIRT3-dependent delactylation of cyclin E2 prevents hepatocellular carcinoma growth. *EMBO Rep* 2023;24:e56052.
14 Pan L, Feng F, Wu J, *et al*. Demethylzeylasteral targets lactate by inhibiting histone lactylation to suppress the tumorigenicity of liver cancer stem cells. *Pharmacol Res* 2022;181:106270.
15 Berger W, Steiner E, Grusch M, *et al*. Vaults and the major vault protein: novel roles in signal pathway regulation and immunity. *Cell Mol Life Sci* 2009;66:43–61.
16 Esfandiary R, Kickhoefer VA, Rome LH, *et al*. Structural stability of vault particles. *J Pharm Sci* 2009;98:1376–86.
17 Tanaka H, Tsukihara T. Structural studies of large nucleoprotein particles, vaults. *Proc Jpn Acad Ser B Phys Biol Sci* 2012;88:416–33.
18 Kolli S, Zito CI, Mossink MH, *et al*. The major vault protein is a novel substrate for the tyrosine phosphatase SHP-2 and scaffold protein in epidermal growth factor signaling. *J Biol Chem* 2004;279:29374–85.
19 Steiner E, Holzmann K, Pirker C, *et al*. The major vault protein is responsive to and interferes with interferon-gamma-mediated STAT1 signals. *J Cell Sci* 2006;119:459–69.
20 Kowalski MP, Dubouix-Bourandy A, Bajmoczi M, *et al*. Host resistance to lung infection mediated by major vault protein in epithelial cells. *Science* 2007;317:130–2.
21 Ben J, Jiang B, Wang D, *et al*. Major vault protein suppresses obesity and atherosclerosis through inhibiting IKK-NF-κB signaling mediated inflammation. *Nat Commun* 2019;10:1801.
22 Mossink MH, van Zon A, Scheper RJ, *et al*. Vaults: a ribonucleoprotein particle involved in drug resistance? *Oncogene* 2003;22:7458–67.
23 Liu S, Hao Q, Peng N, *et al*. Major vault protein: a virus-induced host factor against viral replication through the induction of type-I interferon. *Hepatology* 2012;56:57–66.
24 Frascotti G, Galbiati E, Mazzucchelli M, *et al*. The Vault Nanoparticle: A Gigantic Ribonucleoprotein Assembly Involved in Diverse Physiological and Pathological Phenomena and an Ideal Nanovector for Drug Delivery and Therapy. *Cancers (Basel)* 2021;13:707.
25 Guardavaccaro D, Kudo Y, Boulaire J, *et al*. Control of meiotic and mitotic progression by the F box protein beta-Trcp1 in vivo. *Dev Cell* 2003;4:799–812.
26 Margottin-Goguet F, Hsu JY, Loktev A, *et al*. Prophase destruction of Emi1 by the SCF(betaTrCP/Slimb) ubiquitin ligase activates the anaphase promoting complex to allow progression beyond prometaphase. *Dev Cell* 2003;4:813–26.
27 Tanaka H, Kato K, Yamashita E, *et al*. The structure of rat liver vault at 3.5 angstrom resolution. *Science* 2009;323:384–8.
28 Zhao Z, Shilatifard A. Epigenetic modifications of histones in cancer. *Genome Biol* 2019;20:245.
29 Chen H, Li Y, Li H, *et al*. NBS1 lactylation is required for efficient DNA repair and chemotherapy resistance. *Nature New Biol* 2024;631:663–9.
30 Li W, Zhou C, Yu L, *et al*. Tumor-derived lactate promotes resistance to bevacizumab treatment by facilitating autophagy enhancer protein RUBCNL expression through histone H3 lysine 18 lactylation (H3K18la) in colorectal cancer. *Autophagy* 2024;20:114–30.
31 Li F, Zhang H, Huang Y, *et al*. Single-cell transcriptome analysis reveals the association between histone lactylation and cisplatin resistance in bladder cancer. *Drug Resist Updat* 2024;73:101059.
32 Scheffer GL, Wijngaard PL, Flens MJ, *et al*. The drug resistance-related protein LRP is the human major vault protein. *Nat Med* 1995;1:578–82.
33 Losert A, Lötsch D, Lackner A, *et al*. The major vault protein mediates resistance to epidermal growth factor receptor inhibition in human hepatoma cells. *Cancer Lett* 2012;319:164–72.
34 Liu S, Peng N, Xie J, *et al*. Human hepatitis B virus surface and e antigens inhibit major vault protein signaling in interferon induction pathways. *J Hepatol* 2015;62:1015.
35 Peng N, Liu S, Xia Z, *et al*. Inducible Major Vault Protein Plays a Pivotal Role in Double-Stranded RNA- or Virus-Induced Proinflammatory Response. *J Immunol* 2016;196:2753–66.
36 Rayo J, Gregor R, Jacob NT, *et al*. Immunoediting role for major vault protein in apoptotic signaling induced by bacterial *N*-acyl homoserine lactones. *Proc Natl Acad Sci U S A* 2021;118:e2012529118.
37 Nunes-Xavier CE, Emaldi M, Guldvik IJ, *et al*. Correlation of expression of Major Vault Protein with androgen receptor and immune checkpoint protein B7-H3, and with poor prognosis in prostate cancer. *Pathol Res Pract* 2023;241:154243.
38 Teng Y, Ren Y, Hu X, *et al*. MVP-mediated exosomal sorting of miR-193a promotes colon cancer progression. *Nat Commun* 2017;8:14448.
39 Gondaliya P, Sayyed AA, Driscoll J, *et al*. Extracellular vesicle RNA signaling in the liver tumor microenvironment. *Cancer Lett* 2023;558:216089.
40 Wu X, Hao L, Lin J, *et al*. Unraveling the role of Major Vault Protein as a novel immune-related biomarker that promotes the proliferation and migration in pancreatic adenocarcinoma. *Front Immunol* 2024;15:1399222.
41 Sharma D, Singh M, Rani R. Role of LDH in tumor glycolysis: Regulation of LDHA by small molecules for cancer therapeutics. *Semin Cancer Biol* 2022;87:184–95.
42 Qiao T, Xiong Y, Feng Y, *et al*. Inhibition of LDH-A by Oxamate Enhances the Efficacy of Anti-PD-1 Treatment in an NSCLC Humanized Mouse Model. *Front Oncol* 2021;11:632364.